

We are IntechOpen, the world's leading publisher of Open Access books Built by scientists, for scientists

6,900

Open access books available

185,000

International authors and editors

200M

Downloads

Our authors are among the

154

Countries delivered to

TOP 1%

most cited scientists

12.2%

Contributors from top 500 universities



WEB OF SCIENCE™

Selection of our books indexed in the Book Citation Index
in Web of Science™ Core Collection (BKCI)

Interested in publishing with us?
Contact book.department@intechopen.com

Numbers displayed above are based on latest data collected.
For more information visit www.intechopen.com



New Principles of Monitoring Seismological and Deformation Processes Occurring in the Moon Rock Massive

Olga Hachay and Oleg Khachay

Abstract

Currently, the interest in studying the processes occurring in other planets surrounding the Earth is becoming increasingly important. The Moon-satellite planet is the closest to the planet Earth, and therefore, it makes sense to organize a system for studying it first and foremost, incorporating the most advanced ideas about the physics of processes in rock massive, which are also used in terrestrial conditions. In this paper, new ideas on the organization of seismological and deformation monitoring are set out, based on the results obtained for the rock massive of the Earth and the theoretical ideas presented in the works of I. Prigogine and S. Hawking.

Keywords: Moon rock massive, seismological and deformation processes, new principles of monitoring

1. Introduction

In recent decades, a new science was born—the physics of non-equilibrium processes associated with such concepts as irreversibility, self-organization, and dissipative structures [1]. It is known that irreversibility leads to many new phenomena, such as the formation of vortices, vibration chemical reactions, or laser radiation. Irreversibility plays a significant constructive role. It is impossible to imagine life in a world devoid of interrelations created by irreversible processes. The prototype of the universal law of nature is Newton's law, which can be briefly formulated as follows: acceleration is proportional to force. This law has two fundamental features. It is deterministic: since the initial conditions are known, we can predict movement. And, it is reversible in time: there is no difference between predicting the future and restoring the past; movement to a future state and reverse movement from the current state to the initial state are equivalent. Newton's law is the basis of classical mechanics, the science of the motion of matter, of trajectories. Since the beginning of the twentieth century, the boundaries of physics have expanded significantly. Now, we have quantum mechanics and the theory of relativity. But, as we shall see from the sequel, the basic characteristics of Newton's law—determinism and reversibility in time—are preserved. Is it possible to modify the very concept of physical laws so as to include in our fundamental description of the nature of irreversibility, events and the arrow of time? The adoption of such a program entails a thorough

revision of our formulation of the laws of nature, and it became possible due to the remarkable successes associated with the ideas of instability and chaos [1, 2].

Returning to the results obtained for unstable mountain terrestrial massive, we can note that monitoring studies should be conducted in an active mode, i.e., there should be a source of excitation (seismic or of other nature), and the response of the rock massive is recorded for a not very long time; then, the effect should be repeated, and for this process, as a result, phase diagrams of the rock massive can be constructed.

2. The structure, composition, state, and some methods of their research and their comparison of the Earth and the Moon

This brief review is based on the book [3]. The Moon, devoid of atmosphere and hydrosphere, is a unique repository of traces of the cosmic history of the planets, the key by which people hoped to penetrate into geological secrets. Long-term ground studies of the Moon using astronomical and astrophysical methods have allowed us to obtain numerous data on the laws of its movement and physical conditions on the lunar surface, but this was not enough. Only the development of space technology made it possible to connect the traditional Earth sciences—geology, geochemistry, geophysics, and geodynamics—with powerful methods of observation and data analysis to the studies of the Moon. Successful flights to the Moon and its photographing at close range allowed, first of all, strengthening the geological exploration of the Moon by analyzing its photographs. The delivery of samples of lunar matter opened up unprecedented possibilities for studying the age and composition of the rocks of the Moon using geochemistry methods and allowed to establish the sequence of events in the evolution of the Moon. The first soft landing on the Moon, carried out in 1966 by the Soviet automatic station Luna-9, opened a period of active research directly on the surface of the Moon. The Soviet automatic stations were the first to perform a soft landing in the sea and continental areas of the Moon, photographing the surface, measuring the density and strength of lunar soil, drilling the surface layer, and measuring the physical properties of the soil along long profiles.

Measurements of mechanical as well as some other physical characteristics of the soil at various points on the lunar surface were carried out by American automatic stations “Surveyor.” A large complex of observations on the surface, the selection and delivery of lunar samples, and the measurement of the physical fields on the Moon were made by the American Apollo space missions. The book [3] summarizes the history, methods, and results of complex physical studies of the lunar soil, the crust, and the deep depths of the moon, carried out in the past 40 years. An analysis of all the accumulated data made it possible to assess the state of the substance of the Earth’s interior, its composition, and evolution features and compare the properties of the Earth and the Moon. The mining of deeply hidden underground minerals, the prediction of earthquakes and volcanic eruptions, and the preservation of the ecological balance in nature are currently important tasks facing humanity. For this, it was necessary to understand the Earth and to reveal the secrets of its history and device. Geophysics helps to penetrate into its supercompressed and red hot depths. However, not all problems can be solved while on Earth.

We practically do not analyze here data concerning the composition and age of the rocks of the Moon; this important and extensive topic requires special consideration. Conversely, the entire sections were allocated to describe lunar soil studies, which were carried out according to a special technique, in large volumes, and are of great scientific interest both in terms of improving space technology and for extrapolating open patterns to great depths [5–10].

The most important information about the structure and state of the lunar interior was obtained thanks to the lunar seismic experiment. It was carried out as part of the Apollo program and consisted of continuous recording of natural moonquakes and meteorite falls using seismometers installed by American astronauts on the lunar surface and also from active research using artificial sources of seismic waves: explosions and impacts when the spacecraft was falling on the surface of the Moon [3, 4]. The first lunar seismometer was installed on July 20, 1969, in the Sea of Tranquility on the visible side of the Moon during the Apollo 11 expedition. It was powered by solar panels and kept a seismic record only during the day at the period from November 1969 to December 1972. The visible side of the Moon created a network of four automatic seismic stations of the same type, which were powered by isotope power plants designed for 10 years of continuous operation. Each of these stations was equipped with two types of seismometers and an electronic unit. Three long-period seismometers are arranged vertically and horizontally and allow to record seismic waves from distant sources and determine the direction to the epicenter. For a more accurate separation of waves at short distances, a vertical short-period seismometer was used. These seismometers felt negligible displacement of the surface, corresponding in the size of the atom (10–8 cm). On Earth, it is almost impossible to observe with such sensitivity of equipment: microseisms, ocean waves, wind, and industrial mechanism noise. The Moon, due to the absence of the atmosphere, hydrosphere, biosphere, and active internal processes, is an ideal testing ground for ultraprecise seismic surveys.

Lunar seismograms are completely different from those on Earth: the amplitude of recorded seismic oscillations increases gradually and decreases even more slowly (the “seismic sound” on the Moon lasts for hours). Records on the vertical and horizontal seismometers are not similar to each other, and there are no clear wave arrivals in the subsequent part of the recording—to isolate them; one has to resort to various methods: use narrowband frequency, polarization filters, etc. For these initially fascinate features of the lunar seismograms, an explanation has been received. The fact is that the upper layer of the Moon is very heterogeneous and broken by cracks due to meteorite falling. Seismic signals, scattered on these heterogeneities, stretch “in time” and are destroyed. At the same time, due to the absence of air and water on the Moon, the heat loss of elastic energy is not large, and, conversely, the so-called seismic quality factor is large—therefore, the oscillations do not damp out for a very long time. The features of seismic wave propagation in such a heterogeneous medium are fairly accurately described by the diffusion theory equations. Using these equations, the following estimates of the properties of the lunar scattering layer were obtained: its effective thickness is 15–25 km, and the size of heterogeneities is 2–5 km (and the degree of heterogeneity decreases with depth). Among the natural seismic events on the Moon emit tidal, thermal, and tectonic moonquakes, as well as the fall of meteorites. Seismologists have developed criteria for recognizing the nature of an event by the type of its record, similar to those used on Earth to identify earthquakes and nuclear explosions.

The absolute majority of all seismic phenomena on the Moon (about 90%) are relatively rare, regular, very weak tidal moonquakes with very deep focuses. At present, seismic data obtained using lunar seismometers for the period from November 1969 to July 1972 have been analyzed. During this time, about 5400 seismograms of tidal moonquakes were recorded. On average, about 600 such moonquakes are recorded annually in the Ocean of Storms at the Apollo 12 station, 650 in the Apennines (Apollo 15), 1500 in the region of Fra Mauro (“Apollo 14”), and about 3000 in the area of the Descartes crater (“Apollo 16”). The difference in the number of similar seismic phenomena recorded by the stations is explained by the ground conditions: there are more moonquakes where the upper layer of the

soil and the underlying elastic rocks—breccias—are more powerful. All stations recorded an average of about 700 tidal moonquakes per year. All tidal moonquakes are very weak. The energy released in their focuses is 10^7 – 10^9 erg. The conditional magnitude of the event, adopted in seismology—the magnitude—for tidal moonquakes is 0.5–1.3, whereas for the strongest earthquakes, it reached 8.5. On Earth, earthquakes, as weak as tidal moonquakes, cannot be distinguished against the background of more intense microseisms. If we sum up the energy of all known tidal moonquake sources and assume that the seismicity on the reverse side is not higher than in the Descartes region, then we get the total seismic energy consumption of tidal moonquakes per year equal to 10^{10} – 10^{12} erg. This is more than trillions of times less than earthquake energy. The curves of the number of moonquakes and the amplitude of ground oscillations in a seismic wave, equivalent to the “frequency patterns” of earthquakes, show the strength of the greatest tremors, as well as the number of the weakest shocks. The slope for moonquakes curve is 1.5–3.7 times steeper than for tectonic earthquakes. This means that the Moon is designed in such a way that many weak seismic shocks occur in it and strong ones are impossible. Similar dependences on Earth are obtained for small-scale volcanic earthquakes, as well as for underwater earthquakes in the regions of the middle oceanic ridges. Due to the fact that the seismic stations on the Moon are located at the vertices of a triangle with sides of about 1000 km, it is possible to determine both the position of the epicenter and the depth of the moonquake source. However, due to the small number of stations, the accuracy of such determinations is small (50–100 km). For all focuses, the form of recording remains constant throughout the observation period. According to this property, 41 focal zones were allocated, coordinates of epicenters were determined for 27 of them, and focal depths for 18 of them. The epicenters are grouped into two narrow extended seismic belts. The first is located approximately along the meridian (20–30° W longitude); it starts at 30° south latitude and stretches 2000 km to 40° S. latitude (expanding from 100 km in the north to 200–300 km in the south). The second belt, which is more than 300 km wide, stretches for 1800 km from the center of the visible side of the Moon to the east-northeast. Near its continuation there is a single epicenter fixed on the far side of the Moon. Some connection between the position of the epicenters and the features of the lunar relief is planned. The epicenters of the first seismic belt, comprising half of the focus and 63% of the total number of moonquakes, run along the western edge of the Seas of Rains, Cognized, and Clouds (and even slightly deviate to the east along the contour of the Sea of Clouds). At the same time, 50% of the number of moonquakes occurs on a 700-km stretch in the area of the junction of the Ocean of Storms with the Seas Cognized and the Clouds. More than half of the epicenters of the second seismic belt also fall to the margins of the lunar seas: two are in the south of the Sea of Clarity, two are in the north and east of the Sea of Crises, and three are in the mountain regions separating the Seas of Clarity and Tranquility. All tidal moonquakes occur deep in the depths of the Moon. This is evidenced by clear phases of transverse waves, large amplitude of the first arrivals, a shorter rise time of amplitudes than seismic phenomena of impact origin, and a relatively simple waveform in the interval between the arrivals of longitudinal and transverse waves. Focuses are located at depths of 400–900 km; however, >85% of them fall within a narrower interval—600–800 km. The stability of the form of records of moonquakes from one source (for one station) means that the size of the source zone is no more than 10–20 km. The zone of the epicenter of tidal moonquakes has a complex relief. The rise of focuses in the northern, southern, and central parts of the first seismic zone is planned. In the second zone, the deepest foci are located, and the western half has great depths. In general, the maximum depths of the focuses fall on the equatorial region (including the source on the far

side of the Moon), while the minimum depths correspond to the central part of the southwest quarter of the visible side of the Moon [8].

A strict order is observed in the sequence of tidal lunar storms—an increase in the number of moonquakes after 13, 27, and 206 Earth days. An even longer (6-year) variability in the number of tidal moonquakes, which managed to manifest itself only in the longest series of observations at the Apollo 12 station, is also assumed. The maximum number of moonquakes occurred in the first half of 1970, then a smooth decrease in activity was observed, and in 1972, the Moon was the most passive. The next rise in seismicity was expected in 1976. The observed periodicity of moonquakes can be decoded based on the laws of rotation and motion of the Moon in the gravitational fields of the Earth and the Sun [9]. The orbit of the Moon is hardly one of the most complex planetary orbits. The Moon rotates around the Earth in an ellipse with an average distance of 384 thousand km and with an average eccentricity of the orbit of 0.05. The period of its circulation is 27 and 32 Earth days, during the same time the full rotation of the Moon from west to east around the axis takes place. The lunar equator has a slight slope to the ecliptic and lunar orbit. In the system, Earth-Moon tidal forces act. Viscosity of the planets effects on the dissipation of tidal energy. In addition, the gravity of the Sun causes periodic variations in the lunar orbit, manifested in changes in the eccentricity and distance of the Earth-Moon in the perigee. As a result of all this, a characteristic feature arises—the physical libration of the Moon, which complicates its movement and rotation [11]. It has a latitudinal component with a period of 6 years and a longitude of 206 days.

Initially, when studying tidal moonquakes, it seemed that their tremors were timed to the moments of the apogee and perigee of the Moon in the orbit around the Earth. As data accumulated, it turned out that the picture is more complicated: the peaks of seismic activity are shifted in accordance with the periods of the Moon's libration. At the same time, the seven-month maximum of seismic activity is tied to the greatest eccentricity of the lunar orbit.

Based on the above, none of the researchers of the seismicity of the Moon now doubts the external, cosmic nature of tidal moonquakes—the role of the “trigger mechanism” in them is played by the forces of gravity of the Earth and the Sun. The problem of forecasting planetary shocks, so complex and important on Earth, on the Moon is solved simply—the “schedule” of tidal moonquakes can be made on the basis of the laws of celestial mechanics. For example, the dependence of the moment of seismic shock in the corresponding epicenter on the position on the Moon's surface of a point lying on the straight line connecting the centers of mass of the Earth and the Moon is noted. So, tidal moonquakes can be predicted, but is it so important? After all, they are extremely weak and harmless, and, in particular, future designers of lunar cities and rocket tracks will not need to introduce corrections for the seismic resistance of structures into their calculations.

Tectonic moonquakes. The seismic experiment on the Moon was mainly focused on the detection of tectonic moonquakes; therefore, the stations were established in the contact areas of large-scale surface structures. However, for the entire time of observations, only 11 shocks were recorded, possibly of a tectonic nature. But despite their small amount, they raise the total seismic energy of moonquakes by several orders of magnitude (up to 10^{15} erg). The first characteristic feature of such events is the high frequency of their records (according to this feature, they differ sharply from both tidal moonquakes and meteorite strikes). The arrivals of the longitudinal and transverse waves are very clear, which indicates a small scattering of waves near the source. The slope of the “repeatability curves” is much smaller than that of tidal and thermal moonquakes and closer to earthquakes. The energy of tectonic moonquakes is several orders of magnitude higher than that of tidal moonquakes; their magnitude reaches 4. All detected tectonic moonquakes were

out of the network of lunar seismic stations at distances greater than 600 km: 10 out of 11 were recorded by all stations, and for 4 out of 11, only the azimuth and distance were determined, for 7 events (with an accuracy of 5°). All the epicenters are located on the periphery of the border of the visible and reverse sides of the moon: 9—on the visible and 2—on the back (without an explicit connection with the surface structures). Tidal tectonic moonquakes are not found in the southeast quarter of the visible side of the moon. They are not regular; their form of recording is not repeated. The depth of the foci is not determined precisely; according to the nature of the recording of one of the strong tectonic moonquakes, the lower estimate of the depth of its source—300 km—was obtained, while the foci are deeper than the scattering layer of the crust with a thickness of 25 km.

During the Apollo expeditions, seismic studies of the structure of the subsoil of various scales were carried out: seismic exploration of the upper part of the section, sounding of the crust, and seismic scanning of the mantle. The first detailed study of the velocity of longitudinal waves in the lunar soil was carried out in the Fra Mauro area during the Apollo 14 expedition. Three seismometers recorded astronauts tapping on the ground at a distance of 100 m. More distant points were obtained during the takeoff of the lunar cabin and with the help of special grenades that were blown up after the astronauts departed on command from Earth. A similar experiment was conducted by Apollo 16 astronauts in the continental region of the Descartes crater. Depths of up to 200 m were studied. Finally, during the Apollo 17 expedition in the area of Taurus-Littrow, it was possible to “light up” the structure of the upper layers to a depth of 1.5 km. According to the records at the seismological stations of the fall of the spacecraft, the propagation speeds of transverse seismic waves were determined. As a result of all studies, it was established that the upper part of the Moon consists of separate layers in which the speed of seismic waves increases abruptly with depth. The upper two layers have properties similar in different regions, distant from each other and folded in different breeds. This is due to their identical origin: the scatter of debris during the impact of large meteorites and their subsequent crushing by small ones. Characteristics of lunar soil (regolith): power (2–12 m), velocity of longitudinal waves (90–115 m/s), velocity of transverse waves (35–37 m/s), ratio of velocities of longitudinal and transverse waves (2.7–2.9), Poisson’s ratio [2] (0.42–0.43), density (1.5–1.6 g/cm³), and porosity (more than 50%). In the layer of detrital material (breccias), the power is 18–38 m, the velocity of the longitudinal waves is 300 ± 50 m/s, the ratio of the velocities is 2.2–2.4, the Poisson’s ratio is 0.37–0.40, and the density is 1.7–1.8 g/cm³. Compared with the Earth’s soil, the Moon has very low velocities and a high ratio of velocities (a large Poisson’s ratio).

2.1 Probing of the crust

The lunar crust was studied in the southeastern part of the Ocean of Storms, where the Apollo 12 and 14 seismic stations were located 180 km away. In this case, a rather unusual (for the Earth) method of exciting elastic waves was used—dropping the spent compartments of spaceships. The Apollo expeditions produced two seismic shocks on the surface of the moon. The first shock was, when the third stage of the Saturn-5 rocket weighing more than 14 tons was sent on command from the Earth to a given point on the surface of the Moon. With an almost vertical fall at a velocity of 2.5 km/s at the surface, seismic waves of such force were excited as in the explosion of 10 tons of TNT. The second shock was caused when the takeoff stage, after the crew returned to the main compartment, was dropped near the corresponding seismic station. With a mass of 2.4 tons, the velocity at the surface of 1.7 km/s, and the “gentle” approach trajectory to the surface, the impact of the

lunar cabin was equivalent to an explosion of 800 kg of TNT. The network of lunar seismic stations recorded nine such “artificial” impacts, as well as one natural attack from a meteorite weighing more than 1 ton, which “successfully” fell (May 13, 1972) 140 km north of the seismic station Apollo 14. A total of 14 seismograms were received, 9 of them at a source-receiver distance of 67–358 km and 5 at a distance of 850–1100 km. Seismic records were analyzed in accordance with the methods adopted in the practice of terrestrial deep seismic sounding of the crust. Due to the insufficient accuracy of observations and errors in determining the arrival time of the waves on the seismograms, the velocity structure of the lunar crust was determined with some approximation. In the upper third of the crust, the velocity of longitudinal seismic waves rapidly increased from values of 100 m/s in regolith to 4.5–5.0 km/s at a depth of 10 km and 5.5–5.8 km/s at a depth of 20 km. In the lower part of the crust, the velocity of seismic waves remains almost stable—7.0 km/s. However, only apparent stability is possible, because the lower layers of the crust are “illuminated” so inaccurately even on more detailed observations on Earth that it is sometimes difficult to distinguish a slight increase in the velocity of seismic waves from its gradual decrease. In the mantle of the Moon, the velocity of seismic waves increases abruptly to values of 8 km/s and more. The boundary of the crust-mantle, analogous to the boundary of Mohorovich on Earth, has not yet received on the Moon. The nature of the transition from the crust to the mantle remained unclear, until analysis of their amplitudes and spectra was added to the analysis of the travel times of the waves. The bursts of waves in the subsequent part of the record, identified as reflections from the crust-mantle boundary, showed that this is, in fact, not a boundary, but a transition layer with a thickness from 3–4 to 10–12 km. In some interpretations, a sharp increase in the velocity inside the crust from 5.8 to 6.8 km/s at a depth of 25 km is assumed. In the future, we will be interested in the state of the upper part of the lunar crust, so in the review we omit the results obtained by the structure of the mantle and the core of the Moon. Seismic observations make it possible to determine not only the propagation velocity of longitudinal and transverse waves but also a measure of the proximity of real matter to the model of ideal elasticity—the degree of energy absorption due to irreversible heat losses along the path of the seismic waves. The seismic quality of lunar rocks was estimated in several ways: laboratory (measurements on samples placed in a vacuum), theoretical (comparison of seismograms with calculations), and experimental (measurement of the law of decreasing amplitudes on seismograms). In the latter method, attenuation of the amplitudes of seismic recording was considered depending on time, distance, and frequency. Different definitions gave consistent results. According to the new data, the layered structure of the Moon is distinguished by the seismic quality factor. In the upper layer (regolith), the quality factor for longitudinal waves is 100–300, and in the scattering layer of the crust—3000–5000, in the entire 500-km thickness of the lithosphere—5000 (according to some definitions—7000–10,000), deeper the quality factor drops to 3500 (at a depth of 600 km), 1400 (950 km), and 1100 (1200 km). In the asthenosphere of the moon, the Q on longitudinal waves does not exceed 500. According to the amplitudes of the transverse waves, the seismic Q of the upper 300 km sequence is estimated at 4000; in the 500–800 km layer, it decreases to 1500, and in the asthenosphere, it drops another 10–15 times.

2.2 Lunar mascons

A detailed study of the field of gravity of the Moon became possible after the launch of space satellites into the orbit of artificial satellites of the moon. Observations of satellite orbits were carried out with the help of three ground stations. The first constructions of the picture of the gravitational field of the Moon

were carried out by Soviet researchers on the results of the flight of the Luna-10 spacecraft, and further data were updated on observations of the orbits of artificial satellites of the Lunar Orbiter series, as well as on those sections of the Apollo spacecraft routes, their orbits around the Moon were determined only by its field of gravity. The gravitational field of the Moon turned out to be more complicated and heterogeneous than the Earth, the surface of equal potential of gravity is more uneven, and the sources of anomalies are located closer to the surface of the moon. A significant feature of the lunar field of gravity was the large positive anomalies associated with round seas, which were called mascons (from the English—"mass concentration"). When approaching the mascon, the satellite velocity increases; after passage, the satellite slows down slightly, with the orbit altitude changing by 60–100 m. At first, mascons were discovered in the seas of the visible side: Rains, Clarity, Crises, Nectar, and Humidity; their sizes reached 50–200 km (they fit into the contours of the seas), and the anomaly values were 100–200 mgal [12]. The anomaly of the Sea of Rains corresponded to an excess mass of about $(1.5-4.5) \times 10^{-5}$ the masses of the entire Moon. Subsequently, more massive mascons were discovered on the border of the visible and reverse sides in the Eastern and Regional Seas, as well as a huge mascon in the equatorial zone of the center of the far side of the Moon. There is no sea in this place; therefore, the mascon is called "Hidden." Its diameter is more than 1000 km; the mass is five times the excess mass of the Sea of Rains. Hidden mascon is able to deflect a satellite flying at an altitude of 100×1 km. The total excess mass corresponding to the positive anomalies of gravity exceeds 10^{-4} the mass of the moon. A number of negative anomalies were associated with the lunar mountains: the Jura, the Caucasus, the Taurus, and the Altai. Anomalies of gravity reflect the distribution of mass of matter in the depths of the Moon. If, for example, we assume that mascons are created by point masses, then their depths should be about 200 km in the Sea of Rains, 280 km in the Sea of Clarity, 160 km of Crises, 180 km of Calmness, 100 km of Plenty, 80 km of Sea of knowledge, and 60 km of Ocean of Storms. Thus, gravity measurements found a nonuniform density distribution in the upper mantle.

2.3 Electrical conductivity

None of the lunar expeditions did directly measure the electric field of the moon. It was calculated from the variations of the magnetic field recorded by magnetometers at the Apollo 12, Apollo 15, Apollo 16, and Lunokhod-2 stations. The Moon is devoided of the magnetosphere, but during the magnetosphere, with its rotation around the Earth periodically turns out to be in full Moon in the unperturbed Earth magnetosphere, in the new Moon in the solar wind, and twice for 2 days in the transitional one-shock layer. Fluctuations of an external interplanetary magnetic field penetrate the Moon and induce an eddy current field in it. The rise time of the induced field depends on the distribution of electrical conductivity in the lunar interior. Simultaneous measurements of the external alternating field over the Moon and the secondary field on the surface allow us to calculate the lunar conductivity.

The Moon is arranged "conveniently" for magnetic-telluric sounding. The interplanetary magnetic field, extended from the Sun, is uniform; its front can be considered flat, and therefore for research, as on Earth, a network of laboratories is not necessary. Due to the fact that the Moon has a higher electrical resistance than the Earth, two hourly observations are enough for its sensing, whereas annual Earth winds are needed on Earth. The solar wind flowing around the Moon, having high conductivity, seems to envelop the Moon without letting it out to the surface fields. Therefore, on the solar side of the Moon, only the horizontal component of the alternating magnetic field can be used, whereas on the night side, where the

vertical component works, the situation is more similar to that of the Earth. The Apollo magnetometers recorded the Moon's response in the solar wind on the night and day sides, and also in the geomagnetic plume, where the plasma effects of the solar wind are minimized. In the crater of Lemonier on the solar side of the Moon, on the Lunokhod-2, the solar fluctuation magnetic field was registered. In this case, the horizontal component of the magnetic field reflects the depth electrical conductivity of the Moon, and the magnitude of the vertical component for a long time characterized the intensity of the external field of the Moon. An experimental graph of apparent resistivity was interpreted by comparing with theoretical curves. Soviet (Vanyan et al. [13]) and foreign researchers constructed various models of the electrical conductivity of the Moon. Differing in some details, they give generally similar distributions of the electrical properties of lunar material with depth: in the upper 200 km, there is a poorly conducting layer with a specific resistance of more than 10^6 ohm m; a layer of reduced resistance (10^3 ohm m) with a thickness of 150–200 km is deposited deeper, and the resistance increases by an order of magnitude to 600 km and then decreases again to 10^3 ohm m at a depth of 800 km.

The electrical sensing of the Moon carried out so far reveals the following main features: The Moon as a whole has a higher resistance than the Earth. On top of it is a powerful insulating layer; with depth the electrical conductivity grows. The radial separation of the Moon was found, and a heterogeneity in the horizontal direction was noted with respect to electrical resistance. The temperature inside the Moon was estimated for different compositions of the mantle using the electrical conductivity profiles and the dependence of conductivity on temperature. In all cases, to a depth of 600–700 km, the temperature lies below the melting point of basalt and at great depths reaches or exceeds it.

2.4 Moon's crust

Like on Earth, the Moon has a crust separated from the mantle by a sharp boundary. The thickness of the lunar crust in the southeastern part of the Ocean of Storms (60–65 km) is the same as in the Pamir or Himalayas and more than just oceanic (7–10 km) but also continental crust (40 km). The lunar crust is one-thirtieth of the size of the moon, and thus, in relation to the radius of the planet, it is five times thicker than the average crust. Seismic measurements, which give the most accurate estimates of crustal thickness, have so far been carried out only in the Ocean of Storms. According to other, especially gravimetric, data, we can conclude that the thickness of the crust in different areas is different: in the eastern hemisphere, as well as on the reverse side of the moon, the crust is several times more powerful than in the western. It is possible that, in the region of the Mascon Sea of Crises and Clarity, the denser subcrustal matter lies closer to the surface, here the thickness of the crust decreases to 70–80 km. The difference in the physical properties of the crustal rocks in different areas is noted not only in terms of seismic wave velocities and rock densities—they are differently magnetized and have different electrical conductivities.

Horizontal heterogeneity of densities leads to stresses that cause tectonic moonquakes at depths of 25–300 km. These stresses ($100\text{--}200\text{ kg/cm}^2$) are tens of times smaller than the horizontal forces that determine the tectonic activity of the Earth's lithosphere; therefore, tectonic moonquakes are so weak compared to earthquakes. In the light of new knowledge about the deep structure of the Moon, the picture of the preparation of moonquakes looks like this. Under the action of the forces of gravity of the Earth and the Sun, large tidal voltage drops occur in the moon. They concentrate on the contact of the hard outer and heated inner zones of the moon. This contributes to a complex, contrasting relief of the transition zone. Perhaps, the position of the epicenters of moonquakes reflects the direction of convective flows of matter in the

asthenosphere. At the moments of increasing the attraction of the Moon by the Earth and the Sun, hot fluids and gases are injected into the transitional zone by pulses. They form a kind of “lubricant,” which further facilitates the movement of blocks along the gap at the time of the moonquake. The dimensions of the foci, the intervals between the tremors, and their energy agree quite well within the framework of a theory describing the process of an earthquake as a rapid “ripping up” of cracks in weakened zones. On the Moon, breaks occur within homogeneous blocks of poorly cemented material. Therefore, from push to push, the shape of oscillations in the waves from each source is so well preserved. Because of the small size of the blocks, the shaking is not great. And their “schedule” is fully regulated by the gravitational “pointer” of the Earth and the Sun. There is not enough time for stresses to accumulate, as the next stress impulse and “lubrication” from the asthenosphere arrive—a weak moonquake occurs. Tidal forces of the Earth make the Moon shake often and weakly, not allowing it to accumulate forces for a powerful push.

In the article [14], in order to explain the reason for the manifestation of earthquakes of an “explosive” nature, a model of redistribution of lithostatic pressure during the formation of arch (anticlinal) structures of the Earth’s crust was proposed. It is shown that in the castle part of the formed arch structure, the lithostatic pressure increases significantly, and this leads to a sharp decrease in the volume of the rock (“collapse”). The under locked part of the lithostatic pressure is removed, which leads to mechanical destruction of the rock (“explosion”). It was concluded that the processes of “collapse” and “explosive” destruction of rocks occur during the formation of arch structures and are a possible cause of the manifestation of earthquakes of “explosive” nature. When conducting electromagnetic monitoring in shock-hazardous rock massifs, which were as a result of mining under intense explosive effects in local instability zones, in the section, disintegration zones were found, united by morphology like a vault structure. This may indicate a dynamic hierarchical similarity of the response of the geological environment to the preparation of dynamic manifestations in the form of earthquakes or rock bursts.

3. Informative signs of the preparation of high-energy dynamic phenomena according to the mine seismological monitoring

In order to create a dynamic model adequate to the processes of preparing high-energy processes in the rock massive that are under a strong technogenic impact, it was necessary to use monitoring data in natural occurrence. For this, an analysis of the detailed seismic catalog of the Tashtagol underground mine for 2 years of observations from January 2006 to January 2008 was carried out. The data used are the space-time coordinates of all dynamic phenomena and massive responses that occurred within the mine field during this period, and explosions produced for mining the massive, as well as the values of the explosion energy and massive responses recorded by the seismic station [15]. The whole mine field was divided into two halves: the northwestern section and the west and new capital shaft areas, and the holes from 0 to 13 were designated by us as the northern section. The holes from 14 to 31, the southern ventilation and field drifts, the shaft of the south mine, and the development of the southeastern section are designated as the southern section. All events-responses with horizons with marks –140 m, –210 m, –280 m, and –350 m (maximum depth 800 m) were analyzed. Impacts in the form of explosions were carried out in the southern, southeastern, northwestern, and northern areas. The seismological catalog was also divided into two parts: the northern and southern, according to the events, responses, and explosions that occurred in the northern and southern parts of the mine field.

Phase portraits of the state of the massive of the northern and southern sections are constructed in coordinates $E_0(t)$ and $d(E_0(t))/dt$, t —time, expressed in fractions of 24 h and E_0 —massive seismic energy in J. In the paper [15], morphology of the phase trajectories of the seismic response to explosive effects at various successive intervals of the southern section of the mine is analyzed. During this period, according to the data on the technological and mass explosions produced, most of the energy was pumped into the southern section of the mine. In addition, at the end of the year 2007, it occurred in the southern section, the one of the strongest rock bursts in the entire history of the mine. As a result of the analysis, the characteristic morphology of the phase trajectories of the massive response that is locally in time in a stable state is highlighted. On the phase plane, there is a local area in the form of a coil of interlaced trajectories and small emissions from this coil, not exceeding in energy the values of 10^5 J. At some intervals, this release exceeds 10^5 J, reaching 10^6 J and even 10^9 J [15, 16]. Obviously, there are two interdependent processes: the process of energy accumulation, which is reflected in the region attracting phase trajectories, and the process of resonant discharge of accumulated energy. It is interesting to note that after this reset, the system returns again to the same region attracting phase trajectories. This is confirmed by the detailed analysis of the phase trajectories of the seismic response of the massive before and after the strongest rock burst. However, the process of changing the state of the massive is strongly influenced by the process of a fairly regular external influence in the form of explosions of different powers. During the time between the explosions, the massive does not have time to allocate the energy received by it, which leads to a response delay and nonlinearity of its manifestation, which makes it difficult to predict the time of a highly energetic destructive event [17].

Based on the ideas presented in [18], the analyzed database was supplemented with data of spatial coordinates of explosions. On this basis, a new algorithm for processing seismological information of a detailed mine catalog was developed taking into account the kinematic and dynamic characteristics of deformation waves propagating at different velocities in the rock massif under intense external influence in the form of mass or technological explosions [19]. It was found that waves propagating at velocities from 10 to 1 m/h are the primary carrier of energy in the array and contribute to its release. Events occurring in the array with these speeds and having energy emissions less than 10^4 J contribute to the creep reorganization of the hierarchical inclusions of block parts of the array, which leads to the organization of a new section of dynamic instability. Events occurring in the array with these speeds and having an energy release greater than 10^5 J can be used as precursors which should be taken into account when adjusting the product of explosions in one or another part of the array. The complete absence of these events indicates an increase in the stress state in the massif of the mine as a whole.

3.1 Algorithm for processing seismological information to determine the informative features of the preparation of high-energy dynamic phenomena

In the present work, quantitative estimates have been made of the lag parameter of the high-energy response of the array to a number of anthropogenic impact, during which a significant part of the time was the absence of response of the array. Shock (Sh.36) with an energy of $8.14E+08$ J happened at 25.11.2007 with coordinates $x = 11,928$ m, $y = 11,627$ m, and $z = -264$ m ($+(-450)$ m). It is marked, like all the rest of our studied responses, which occurred in the southern part of the mine with the letters Sh. and number 36. Explosions are designated as (i), where i is the number of the explosion for the period 2006–2008. We have obtained additional

estimates of the distances from the explosion point to the response point of the massif. The coordinates of the explosions and massif responses are taken from the seismic mine catalog of the Tashtagol mine.

3.2 Discussions

As follows from the analysis of the data in **Tables 1–4** and **Figures 1–4**, the response of the massif Sh.36 in the form of a high-energy response only appears, starting with the distances between the point of impact and the response from 100 m to 200 m. At the same time, the lag time of the massif response to the impact occurred in the form of a rock shock is tens and even hundreds of days. Therefore, despite the fact that the Sh.36 response from the impact (78) (**Table 4**) occurred almost instantly,

Imp.-Sh.	dx	dy	dz	r	dt	Eimp	E0
(1)-Sh.1	0	-23	10	25	77	5.40E+04	2.7E+06
(1)-Sh.2	-18	-1	3	18	111	5.40E+04	1.48E+04
(23)-Sh.7	-24	-16	3	29	0.3	2.15E+07	1.56E+04
Sh.10–Sh.17	-20	17	-18	32	40	1.17E+04	1.56E+04
Sh.10–Sh.18	-21	-31	-13	40	48	1.17E+04	1.56E+04
(38)-Sh.17	-30	-24	-1	38	28	7.97E+03	1.56E+04
(46)-Sh.21	-25	11	3	27	2	9.52E+07	7.48E+04
Sh.31–Sh.32	1	-2	-3	4	0.3	1.10E+04	1.04E+04

Imp, impact; Sh, response; dx, dy, dz, difference of Cartesian coordinates of the points of impact and response in m; $r = \sqrt{dx^2 + dy^2 + dz^2}$, the distance (m) between the point of impact and the point of response; dt, time difference of impact and response points in 24 h; Eimp, impact energy (J); E0, energy response (J).

Table 1.

The impact and the response of the mine southern part massif within the distance from 0 m to 50 m from the points of explosions.

Imp.-Sh.	dx	dy	dz	r	dt	Eimp	E0
(23)-Sh.5	-56	-34	28	71	0.03	2.15E+07	1.24E+04
(30)-Sh.9	55	13	-13	58	18	6.35E+06	1.65E+04
(34)-Sh.10	43	-49	-58	87	2	2.44E+04	1.17E+04
(38)-Sh.11	4	-41	41	58	15	7.97E+03	1.04E+04
(38)-Sh.18	-31	-72	4	78	36	7.97E+03	1.17E+04
Sh.11–Sh.16	26	62	6	67	11	1.04E+04	1.10E+04
(42)-Sh.13	24	-24	-59	68	0.02	1.19E+09	4.04E+04
Sh.15–Sh.19	75	60	18	98	22	2.92E+04	2.44E+04
Sh.23–Sh.28	-7	-62	-39	74	138	2.92E+04	1.16E+04
Sh.25–Sh.27	42	42	-40	72	38	3.74E+04	4.04E+04
(72)-Sh.34	72	54	22	93	42	1.80E+06	8.68E+04
(78)-Sh.35	97	18	7	99	0.1	8.68E+04	2.67E+04

Imp, impact; Sh, response; dx, dy, dz, difference of Cartesian coordinates of the points of impact and response in m; $r = \sqrt{dx^2 + dy^2 + dz^2}$, the distance (m) between the point of impact and the point of response; dt, time difference of impact and response points in 24 h; Eimp, impact energy (J); E0, energy response (J).

Table 2.

The impact and the response of the mine southern part massif within the distance from 50 m to 100 m from the points of the impacts.

Imp.-Sh.	dx	dy	dz	r	dt	Eimp	E0
(16')-Sh.36	111	97	-22	149	575	1.24E+04	8.14E+08
(21)-Sh.36	117	53	-34	133	539	1.65E+04	8.14E+08
(23)-Sh.4	69	-82	19	109	0.01	2.15E+07	1.92E+04
(23)-Sh.8	-28	-121	-2	124	0.06	2.15E+07	3.74E+04
(35)-Sh.36	118	61	34	137	400	1.92E+04	8.14E+08
(38)-Sh.36	77	86	-18	117	393	7.97E+03	8.14E+08
(39)-Sh.36	100	45	33	114	392	2.07E+06	8.14E+08
(41)-Sh.36	102	74	41	132	378	3.95E+06	8.14E+08
Sh.4-Sh.5	-125	48	9	134	0.03	1.92E+04	1.24E+04
Sh.5-Sh.6	-35	-118	-13	124	0.96	1.24E+04	3.35E+05
Sh.7-Sh.8	4	-105	5	105	0.09	1.04E+04	3.74E+04
Sh.20-Sh.21	-95	-28	-81	128	1	6.60E+04	7.48E+04
(43)-Sh.18	13	-88	-46	100	7	1.55E+06	1.17E+04
(43)-Sh.36	121	70	24	142	364	1.55E+06	8.14E+08
(44)-Sh.18	32	-108	17	114	0.08	3.98E+06	1.17E+04
(68)-Sh.33	31	-137	-20	142	70	2.70E+06	3.48E+05
(68)-Sh.36	89	70	34	118	70	2.70E+06	8.14E+08
(70)-Sh.34	106	33	17	112	56	2.06E+06	8.68E+04
(71)-Sh.36	63	75	48	109	49	1.65E+05	8.14E+08
(72)-Sh.36	55	91	39	113	42	1.80E+06	8.14E+08
(78)-Sh.36	80	55	44	107	0.06	8.68E+04	8.14E+08

Imp, impact; Sh, response; dx, dy, dz, difference of Cartesian coordinates of the points of impact and response in m; $r = \sqrt{dx^2 + dy^2 + dz^2}$, the distance (m) between the point of impact and the point of response; dt, time difference of impact and response points in 24 h; Eimp, impact energy (J); E0, energy response (J).

Table 3.

The impact and the response of the mine southern part massif within the distance from 100 m to 150 m from the points of the impacts.

it was preceded by a long process of preparing a resonant energy release [22]. Based on the ideas presented in [18], the analyzed database was supplemented with data of spatial coordinates of impacts. On this basis, a new algorithm for processing seismological information of a detailed mine catalog was developed taking into account the kinematic and dynamic characteristics of deformation waves propagating at different velocities in the rock massif under intense external influence in the form of mass or technological explosions [19]. It was found that waves propagating at speeds from 10 to 1 m/h are the primary carrier of energy in the massif and contribute to its release. Events occurring in the massif with these velocities and having energy emissions less than 10^4 J contribute to the creep reorganization of the hierarchical inclusions of the block parts of the massif, which lead to the organization of a new section of dynamic instability. Events occurring in the array with these speeds and having an energy release greater than 10^5 J can be used as precursors which should be taken into account when adjusting the product of explosions in one or another part of the array. The complete absence of these events indicates an increase in the stress state in the massif of the mine as a whole. In [20], an algorithm for processing seismological information of a detailed mine catalog was developed to determine the informative features of the preparation of high-energy dynamic phenomena. For this purpose, quantitative

Imp.-Sh.	dx	dy	dz	r	dt	Eimp	E0
(23)-Sh.6	-91	-152	15	178	1	2.154E+07	3.35E+05
(29)-Sh.36	170	91	-23	194	434	2.07E+06	8.14E+08
(30)-Sh.36	174	76	2	190	427	6.35E+06	8.14E+08
(34)-Sh.36	130	78	23	153	407	2.44E+04	8.14E+08
(40)-Sh.36	140	63	17	154	385	2.70E+06	8.14E+08
Sh.4-Sh.6	-160	-70	4	175	0.99	1.92E+04	3.35E+05
Sh.20-Sh.37	38	-146	14	152	336	3.35E+05	6.39E+04
(42)-Sh.14	-78	-180	26	198	0.06	1.19E+09	1.92E+04
(42)-Sh.15	163	-38	-31	170	2	1.19E+09	2.92E+04
Sh.13-Sh.15	187	-14	-28	190	2	1.48E+04	2.92E+04
(44)-Sh.36	140	50	50	157	357	3.98E+06	8.14E+08
(46)-Sh.36	140	64	-17	155	336	9.52E+07	8.14E+08
(59)-Sh.36	115	117	1	164	197	1.10E+04	8.14E+08
(74)-Sh.36	98	111	-54	158	35	2.93E+06	8.14E+08
(78)-Sh.33	1	-168	58	178	0.01	8.68E+04	3.48E+05

Imp, impact; Sh, response; dx, dy, dz, difference of Cartesian coordinates of the points of impact and response in m; $r = \sqrt{dx^2 + dy^2 + dz^2}$, the distance (m) between the point of impact and the point of response; dt, time difference of impact and response points in 24 h; Eimp, impact energy (J); E0, energy response (J).

Table 4.
The impact and the response of the mine southern part massif within the distance from 150 m to 200 m from the points of the impacts.

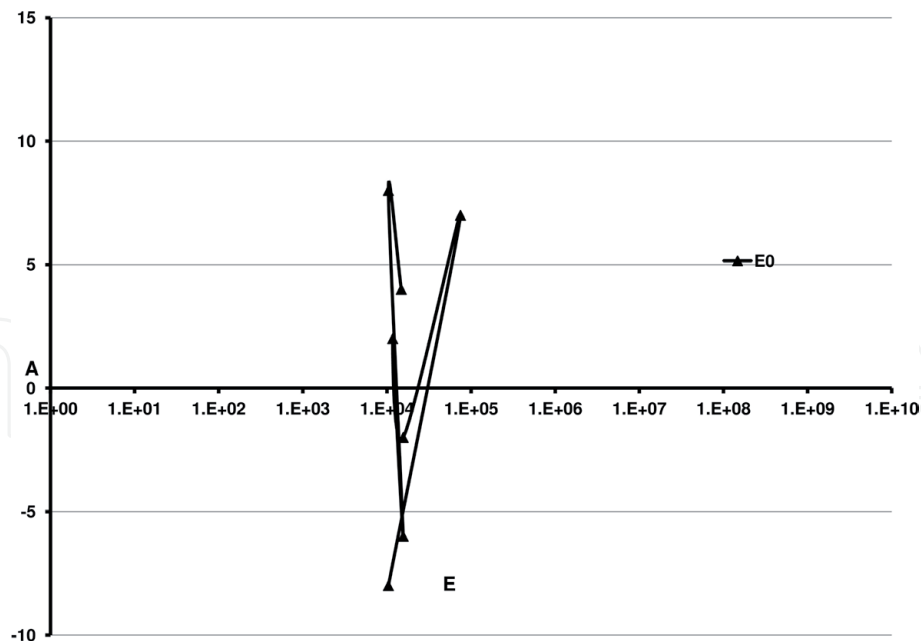


Figure 1.
Phase diagrams of the dynamical state of the massif southern mine part during the period 2006–2008 years, $r = 0 \text{ m} - 50 \text{ m}$. Horizontal axe: $E = E_0$; vertical axe: $A = aLgf, f = \left| \frac{\partial E_V}{\partial t} \right|, a = \text{sign } \partial E_V E_V = E_{imp} - E_0$.

estimates have been made of the lag parameter of the high-energy response of the array to a number of anthropogenic impacts, during which a significant part of the time was the absence of the response of the array. Response $8.14E+08 \text{ J}$ happened 25.11.2007 year with coordinates $x = 11,928 \text{ m}$, $y = 11,627 \text{ m}$, and $z = -264 \text{ m}$ ($+(-450 \text{ m})$). We have obtained additional estimates of the distances from the impact

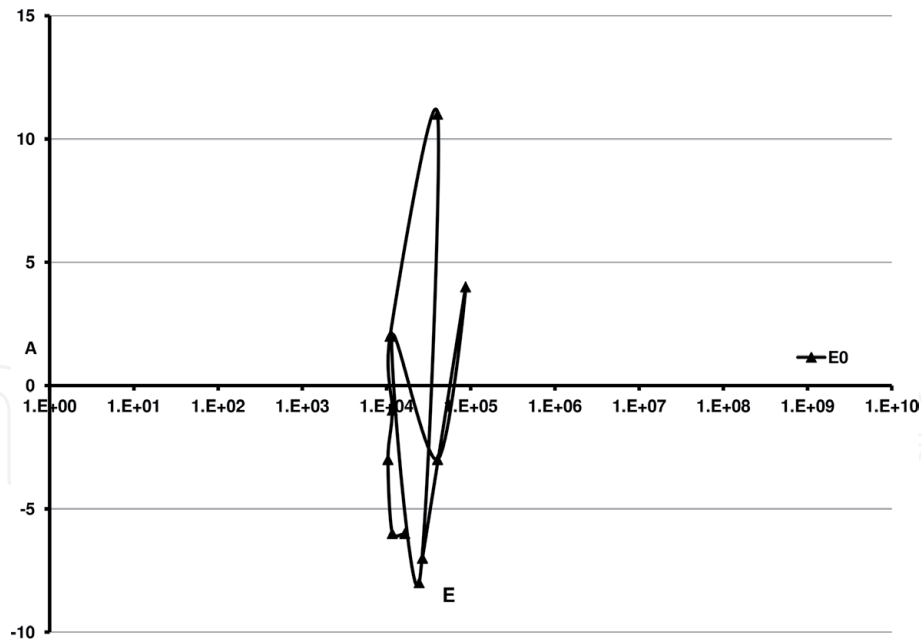


Figure 2.
 Phase diagrams of the dynamical state of the massif southern mine part during the period 2006–2008 years, $r = 50 \text{ m}–100 \text{ m}$. Horizontal axe: $E = E_0$; vertical axe: $A = aLgf$, $f = \left| \frac{\partial E_V}{\partial t} \right|$, $a = \text{sign } \partial E_V E_V = E_{imp} - E_0$.

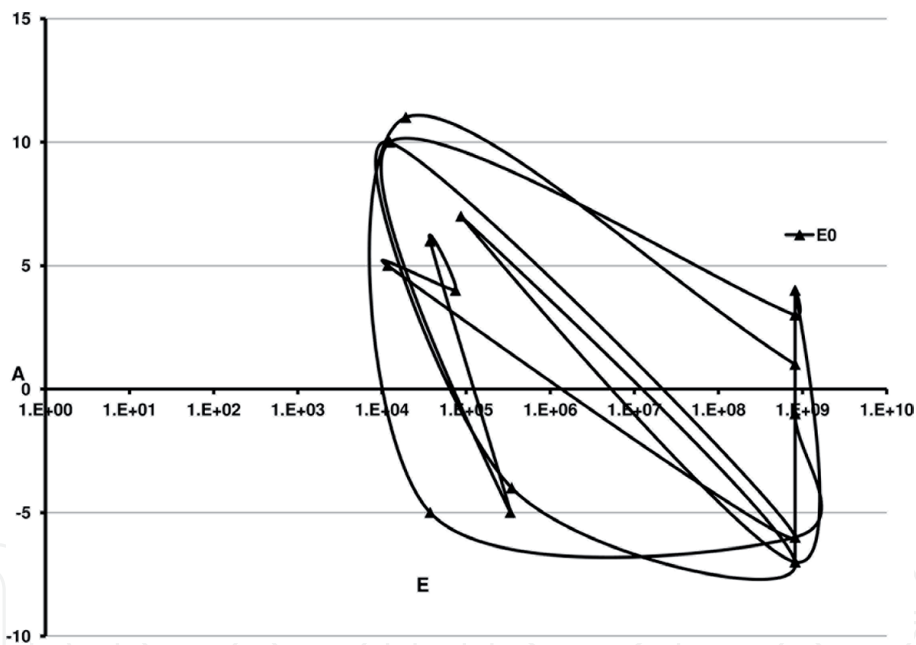


Figure 3.
 Phase diagrams of the dynamical state of the massif southern mine part during the period 2006–2008 years, $r = 100 \text{ m}–150 \text{ m}$. Horizontal axe: $E = E_0$; vertical axe: $A = aLgf$, $f = \left| \frac{\partial E_V}{\partial t} \right|$, $a = \text{sign } \partial E_V E_V = E_{imp} - E_0$.

point to the response point of the massif. The coordinates of the impacts and massif responses are taken from the seismic mine catalog of the Tashtagol mine. As follows from the analysis performed, we can repeat that the massif response in the form of a high-energy response is manifested only from the distances between the point of impact and the response from 100 m to 200 m. At the same time, the lag time of the array response to the impact occurred in the form of an explosion is tens and even hundreds of days. Therefore, despite the fact that the response from the last impact occurred almost instantly [20], it was preceded by a long process of preparing resonant energy release [21], which must be accompanied by electromagnetic monitoring of the occurrence and accumulation of disintegration zones in the massif volume: $dx = 100–180 \text{ m}$, $dy = 33–180 \text{ m}$, and $z = (-210 - (-300)) + (-450) \text{ m}$. It is important

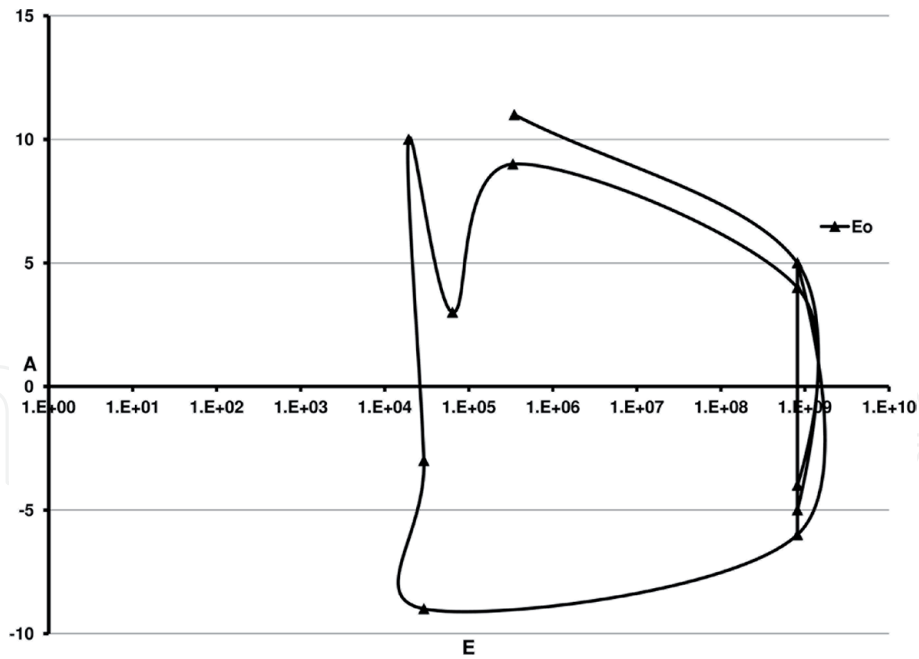


Figure 4.

Phase diagrams of the dynamical state of the massif southern mine part during the period 2006–2008 years, $r = 150\text{ m}–200\text{ m}$. Horizontal axe: $E = E_o$, vertical axe: $A = aLgf$, $f = \left| \frac{\partial E_V}{\partial t} \right|$, $a = \text{sign } \partial E_V E_V = E_{imp} - E_o$.

to take into account not only the direct impact of explosions on this process but also the responses that appear after a while as shocks that contribute to the resonant release of energy. The developed algorithm for processing seismological information of the detailed mine catalog allows extracting additional important information for predicting hazardous phenomena in ore mines and for developing the theory of dynamic phenomena in natural geological, geophysical, and lunar environments.

As a result of the analysis performed in [23], the use of the theory of catastrophe recommendations [24] on the prediction of dynamic phenomena can be drawn from the following conclusions. The processes occurring in mountain massive are dynamic processes that can be controlled following the recommendations provided by the theory of catastrophes. In these processes, the energy values during explosions and the location of these explosions relative to the region of the massif under study or being processed are the control parameters. The internal parameters are the kinematic and dynamic parameters of deformation waves [21, 25–27], as well as the structural features of the massif through which these waves pass [22]. The use of analysis methods for short-term and medium-term forecasting of the state of a mountain massif only by using control parameters is not enough because the massif has sharp heterogeneities. However, the joint use of qualitative recommendations of the theory of catastrophes and the spatial-temporal data of changes in the internal parameters of the massif will allow preventing catastrophes in mountain terrestrial and lunar massive.

4. Conclusions

In the case of studying the state of the lunar mountain massive, it is necessary to organize active seismic and deformation monitoring to the similarity organized on the Earth within unstable mountain massive. Since the Moon is at a considerable distance from the Earth, the active effect as an excitation source can be of electromagnetic or laser type. The basic principle of monitoring should be active and regularly repeated, and then the processing algorithm described above can be used, bypassing the time paradox, to predict the state of the lunar mountain

massive. At present, theoretical results on modeling the electromagnetic and seismic field in a layered medium with inclusions of a hierarchical structure are in demand. Simulation algorithms are constructed in the electromagnetic case for 3D heterogeneities, in the seismic case for 2D heterogeneities [28–30]. It is shown that with an increase in the degree of hierarchy of the environment, the degree of spatial nonlinearity of the distribution of the components of the seismic and electromagnetic fields increases, which corresponds to the detailed monitoring experiments conducted in the shock-hazardous mines of the Tashtagol mine and SUBR. The theory developed demonstrated how complex the process of integrating methods using an electromagnetic and seismic field to study the response of a medium with a hierarchical structure. This problem is inextricably linked with the formulation and solution of the inverse problem for the propagation of electromagnetic and seismic fields in such complex environments. In [31, 32], the problem of constructing an algorithm for solving an inverse problem using the equation of a theoretical inverse problem for the 2D Helmholtz equation was considered. Explicit equations of the theoretical inverse problem are written for the cases of electromagnetic field scattering (E and H polarization) and scattering of a linearly polarized elastic wave in a layered conducting and elastic medium with a hierarchical conducting or elastic inclusion, which are the basis for determining the contours of misaligned inclusions of the l th rank of the hierarchical structure. It is obvious that when solving the inverse problem, it is necessary to use observation systems setup to study the hierarchical structure of the environment as the initial monitoring data. On the other hand, the more complex the environment, each wave field introduces its information about its internal structure; therefore, the interpretation of the seismic and electromagnetic fields must be conducted separately, without mixing these databases. These results should be used when studying the structure and condition of lunar massive of rocks by deep drilling.

Author details

Olga Hachay^{1*} and Oleg Khachay²

¹ Institute of Geophysics UB RAS, Yekaterinburg, Russian Federation

² Ural Federal University, Yekaterinburg, Russian Federation

*Address all correspondence to: olgakhachay@yandex.ru

IntechOpen

© 2019 The Author(s). Licensee IntechOpen. This chapter is distributed under the terms of the Creative Commons Attribution License (<http://creativecommons.org/licenses/by/3.0>), which permits unrestricted use, distribution, and reproduction in any medium, provided the original work is properly cited. 

References

- [1] Prigogine I, Stengers I. Time, Chaos, and Quantum: To Solve the Paradox of Time. Book House LIBROKOM; 2009. 232 p
- [2] Hawking S. From the Big Bang to the Black Holes. A Short History of Time. M. Mir; 1990. Ch. 8
- [3] Galkin IN, Shvarev VV. The Structure of the Moon—New in Life, Science, Technology Series “Astronautics, Astronomy”. No. 2, Knowledge. 1977. 63 p
- [4] Nikolaev AV, Sadovsky MA. New methods of seismic exploration: Development prospects. Herald of the USSR Academy of Sciences. 1982;1:57-64
- [5] Cosmo chemistry of the moon and planets. (ed.) A. Vinogradov M. editor. Science; 1975. 764p
- [6] Kuskov OL. Constitution of the Moon: 3. Composition of middle mantle from seismic data. Physics of the Earth and Planetary Interiors. 1995;90:55-74
- [7] Kuskov OL. Constitution of the Moon: 4. Composition of the mantle from seismic data. Physics of the Earth and Planetary Interiors. 1997;102:239-257
- [8] Frondel J. Lunar Mineralogy. J. Willey & Sons; 1975. 177 p
- [9] Ruskol E. Origin of the Moon. Moscow: Nauka; 1975. 188 p (in Russian)
- [10] Zharkov VN. The Internal Structure of the Earth and Planets. M.: Science; 1983. 413 p
- [11] Gusev A, Hanada H, Petrova N. Rotation, Physical Libration, Internal Structure Multiply Moon. Kazan, Kazan Federal University; 2015. 323 p
- [12] Sagitov MG. Moon’s Gravimetry. M. Science. Main Edition Phys.-Mat. Literature; 1979. 432 p
- [13] Vanyan LL et al. The apparent electrical resistance of the moon and its interpretation. Izv. Academy of Sciences of the USSR. “Physics of the Earth”. 1973;11: 3-12
- [14] Khachay OA, Pogrebnoy VN, Khachai OYu, Malosiyeva MT. Similarity of a possible reason for the manifestation of foci-type earthquake foci and dynamic phenomena in impact-dangerous ore mines. Mining Informational Analytical Bulletin. 2018;4:159-171. DOI: 10.25018/0236-1493-2018-4-0-159-171
- [15] Hachay OA. The study and control of the state of mountain ranges from the perspective of the theory of open dynamic systems. Mining Informational Analytical Bulletin. 2013;7:145-151
- [16] Hachay OA, Khachay AY, Khachay OY. Chapter 5. Dynamic model of the state of the environment. In: Quadfeul S-A, editor. Fractal Analysis and Chaos in Geosciences. Croatia: InTech; 2012. 174 p
- [17] Hachay OA, Khachay AY. The study of the stress-strain state of hierarchical environments. In Proceedings of the Third Tectonophysical Conference at the Institute of Physical Problems RAS; October 8-12, 2012. Moscow: Institute of Physical Problems RAS; 2012. pp. 114-117
- [18] Oparin VN, Vostrikov VN, Tapsiev AP, et al. About one kinematic criterion for predicting the limiting state of rock massifs according to mine seismological data. FTPRPI. 2006;6:3-10
- [19] Hachay OA, Khachay OY. Algorithm for constructing a scenario for the preparation of rock bursts in

rock masses under the influence of explosions according to a seismic catalog. *Mining Informational Analytical Bulletin*. 2014;**4**:239-246

[20] Chulichkov AI. *Mathematical Models of Nonlinear Dynamics*. 2003; M. Phizmatlit. 294 p

[21] Hachay OA, Khachay OY, Klimko VK, Shipeev OV. Informative signs of the preparation of high-energy dynamic phenomena according to mine seismological monitoring. *Mining Informational Analytical Bulletin*. 2015;**4**:155-216

[22] Hachay OA, Khachay OY. Comparison of the features of the synergistic properties of the state of a shock-hazardous rock mass, determined according to seismic and inductive electromagnetic monitoring. *Monitoring Science and technology*. 2014;**3**:50-55

[23] Hachay OA, Khachay OY. The theory of catastrophes is one of the basic components of the analysis of seismic responses of a mountain range to explosive effects. *Fundamental and Applied Issues of Mining Sciences*. 2017;**4**(2):175-181

[24] Arnold VI. *Catastrophe Theory*. 3rd ed. Ext. - M.: Science. Ch. ed. Phys.-Mat. Lit; 1990. 128 p

[25] Hachay OA, Khachay OY, Klimko VK. Dynamic characteristics of slow deformation waves as an massif response to explosive effects. *Mining Informational Analytical Bulletin*. 2013;**5**:208-214

[26] Hachay OA, Khachay OY, Shipeev OV. Study of the hierarchical structure of the dynamic characteristics of slow deformation waves—Response to explosive effects. *Mining Informational Analytical Bulletin*. 2013;**5**:215-222

[27] Hachay OA, Khachay OY. The method of assessing and classifying

the stability of an array of rocks from the standpoint of the theory of open dynamic systems according to geophysical monitoring. *Mining Informational Analytical Bulletin*. 2005;**6**:131-142

[28] Hachay OA, Khachay OY, Khachay AY. New methods of geoinformatics for the integration of seismic and gravitational fields in hierarchical environments. *Geoinformatics*. 2016;**3**:25-29

[29] Hachay OA, Khachay OY, Khachay AY. New methods of geoinformatics monitoring wave fields in hierarchical environments. *Geoinformatics*. 2015;**3**:45-51

[30] Hachay OA, Khachay AY. Simulation of seismic field propagation in a layered-block elastic medium with hierarchical plastic inclusions. *Mining Informational Analytical Bulletin*. 2016;**12**:318-326

[31] Hachay OA, Khachay AY. Determination of the surface of anomalously intense inclusion in a hierarchical layered-block medium according to acoustic monitoring data. *Mining Informational Analytical Bulletin*. 2016;**4**:354-356

[32] Hachay OA, Khachay AY. Determination of the surface of fluid-saturated porous inclusion in a hierarchical layered-block medium according to electromagnetic monitoring. *Mining Informational Analytical Bulletin*. 2015;**4**:150-154